Electrical and plasma parameters of ICP with high coupling efficiency

V A Godyak

RF Plasma Consulting, Brookline, MA 024461, USA

E-mail: egodyak@comcast.net

Abstract
A novel design of ICP with high coupling efficiency is presented. The efficiency augmentation
is achieved using a thin window and an antenna coil enhanced by a ferromagnetic core.
Considerable improvement of ICP electrical and plasma characteristics is demonstrated
through experiments in ICP operated at 2 MHz in a wide range of argon gas pressures between
1 mTorr and 1 Torr, and discharge power between 15 W and 0.5 KW.

(Some figures in this article are in colour only in the electronic version)

1. Introduction

Over the last decade, a large variety of plasma sources based on different mechanisms of electromagnetic power absorption has been considered for large scale semiconductor manufacturing. Capacitively coupled plasmas (CCPs) and very high frequency CCPs (VHFCCPs), inductively coupled plasmas (ICPs) and those enhanced by a ferromagnetic core, helicons, electron cyclotron resonance (ECR) and surface wave (SW) plasmas have been the main rf plasma sources under exploration [1, 2].

The choice of a particular plasma source for commercial reactors is usually based on the expected plasma properties believed to be inherent to a specific method of plasma excitation. In fact, different plasma sources tend to have very similar plasma parameters and rates of plasma processing if the reactor geometry, gas composition, pressure and power delivered to the plasma electrons remain the same [3, 4]. In this respect, the different methods of plasma production do not result in essentially different plasmas, but differ by other features important for particular applications, such as plasma boundary sheaths, plasma uniformity, system efficiency and ability to work over a wide range of power, gas composition and plasma geometry.

Capacitively coupled plasma (CCP) sources operated at 13.56 MHz were the first to be implemented in plasma processing technology. However, their inability to generate large plasma densities at low gas pressures and to separate functions of plasma production and ion acceleration resulted in the implementation of IPC sources in the beginning of 1990s. Plasma reactors based on ICP can provide high density plasma at low gas pressure and independent control of plasma density (ion flux) and ion energy to the processing wafer. Such independent control is provided by separate rf power sources. One is the power source dedicated to driving the antenna coil, while the other is the bias source dedicated to rf biasing of the wafer.

The implementation of ICP in commercial plasma processing reactors has shown some essential limitations of such a processing tool. Those limitations include the inability to work in inductive mode with low plasma densities ($n \ll 10^{11}$ cm^{-3}) and with small plasma gaps, significant radial and azimuthal non-uniformities, as well as capacitive coupling leading to window erosion and plasma contamination. Probably for those reasons, the concept of using a VHFCCP (CCP at a very high frequency, 2–12 times larger than 13.56 MHz) as a power source and biasing the wafer with a relatively low frequency, 2.0–13.56 MHz (dual-frequency CCP), is today the mainstream approach for plasma etching reactors.

The extensive experience with the VHFCCP gained by the plasma processing community and in research laboratories has revealed fundamental problems with the VHFCCP associated with the electromagnetic nature of the VHF field in such reactors when the plasma skin depth becomes comparable to the plasma gap or/and the wavelength, λ, of the electromagnetic field in the slowing wave structure of the VHFCCP (which is a few times less than the wavelength in vacuum, $\lambda_0 = 2\pi c/\omega$ becomes comparable to the plasma radial dimension [5, 6]. Those electromagnetic effects lead to strong plasma non-uniformity, which becomes more prominent at higher operating frequencies, higher plasma densities and larger wafer sizes. Such phenomena stand in
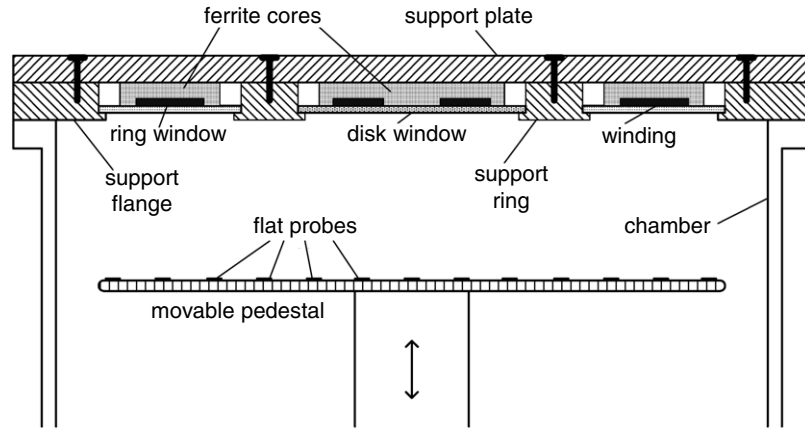
Figure 1. Schematic diagram of the ICP chamber with the antenna block and the pedestal.

the way of the main plasma processing trend, which requires a larger processed area and a higher processing speed.

At very high frequencies and high plasma densities, the electromagnetic effects can overcome the capacitive coupling effect. Then, a parallel plate structure (typical for CCP) operates mainly in inductive mode, i.e. becoming an ICP [7]. Due to the fact that various resonant modes occur for certain relationships between the rf frequency, the plasma size and the plasma density, a VHFCCP of a very high frequency may become unstable, jump from one mode to another and become uncontrollable. Due to these fundamental problems, it seems that plasma reactors based on VHFCCP have no future for processing 450 mm wafers and large solar panels. In addition, VHF rf generators and matching-tuning networks are complex, expensive and of low efficiency.

Recently, there have been many proposals, mainly in patent literature, to improve plasma processing reactors. The following two trends for the considerable improvement of ICP reactors have clearly crystallized: (1) an ICP enhanced by a ferromagnetic core [8–11] and (2) ICPs with distributed rf excitation systems, which have multiple antennas for a uniform spread of plasma over a large processing area [10–12]. In lighting technology, which is far more mature than plasma processing technology, all existing commercial rf light sources are enhanced by ferromagnetic core ICPs, which are more efficient and operate at a much lower frequency than the majority of ICP reactors [13]. The high efficiency of commercial low frequency ICP rf light sources is achieved by strong coupling between the antenna and the plasma, which suggests a third trend for improving ICP plasma processing reactors.

An attempt to combine all of the three trends mentioned above in order to improve the design of ICP is described in this paper. The proposed approach and design of such new ICP sources supported by the results of experimental studies in a wide range of rf powers and gas pressures.

2. ICP design and experimental setup

In conventional ICP reactors with 300 mm processing wafers, the support window diameter is usually 30–50 cm, which

requires a flat window thick enough to withstand atmospheric pressure. The thickness of a quartz window in industrial plasma reactors (depending on the support window diameter) is in the 20–50 mm range. Using a dome-shaped window made of a strong ceramic material allows one to reduce the window thickness two–three times, but leads to a significant increase in the gap between the window ceiling and the wafer.

In this paper, in order to increase the antenna coil coupling to the plasma, the thickness of the dielectric window separating the antenna and the plasma was reduced by one order of magnitude compared with conventional ICP reactors. Simultaneously, to ensure the mechanical integrity of the thin window, the support window distance was also reduced to be considerably smaller than the chamber diameter.

The conceptual drawing of the antenna block placed on the discharge chamber is given in figure 1, which shows the vertical cross section of the ICP chamber with a pedestal and the antenna block installed on the chamber flange. The bottom views (from the plasma side) of the assembled antenna block and view without the support flange, support ring and the windows are shown correspondingly in figures 2(*a*) and (*b*).

The antenna block has a thin ceramic disk and ring windows sitting on the lips of the bottom support ring and aluminum support flange. The 2 mm-thick ring window has a 19.7 cm outer diameter and a 10.7 cm inner diameter. A flat eight-turn coil made of Teflon insulated 18-gauge wire with a 15.2 cm central diameter is placed on the ring window and covered with a ferromagnetic core structure consisting of 13 ferrites tablet pieces with a π-cross section to accommodate the coil. The ferrite pieces are covered by an aluminum support plate bolted to the support flange and support ring, thus assuring the mechanical integrity of the antenna block. The assembled antenna block, which is 24 cm in diameter and 2.6 cm thick, is installed on the discharge chamber with a 20 cm inner diameter, as shown in figure 1.

An axial direction movable disk pedestal of 16 cm diameter, with an array of flat Langmuir probes along its diameter, can be set at the distance $d = 1.5$–8.0 cm from the bottom of the antenna block. The electrical and plasma parameter measurement are made at the fixed pedestal distance of 6 cm. A cylindrical Langmuir probe (movable in the radial
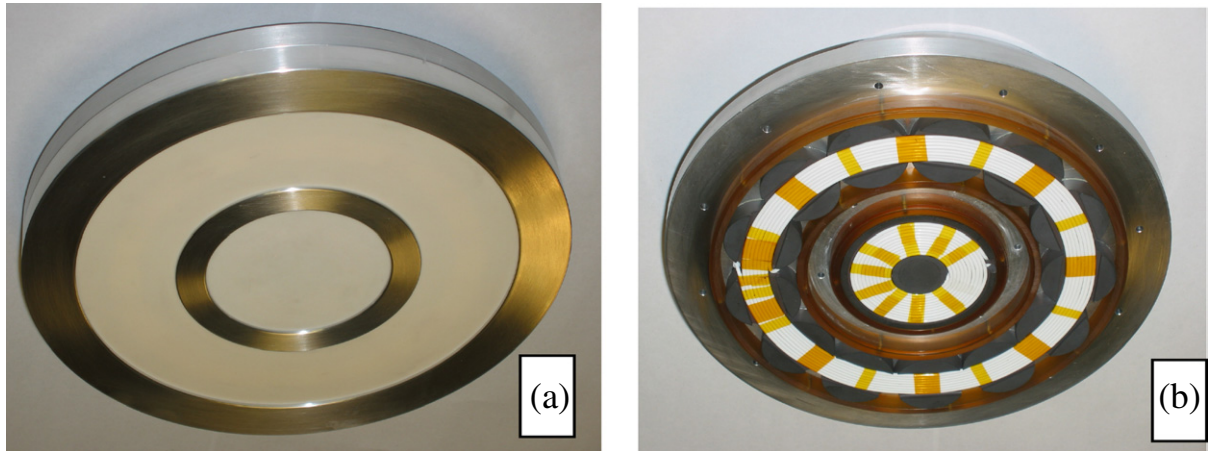
Figure 2. Bottom view of the antenna block.
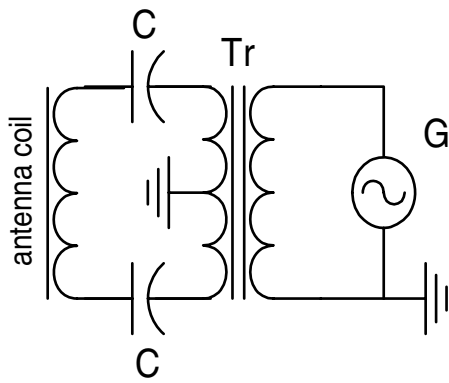
Figure 3. Symmetric matching network with the matching transmission-line transformer.

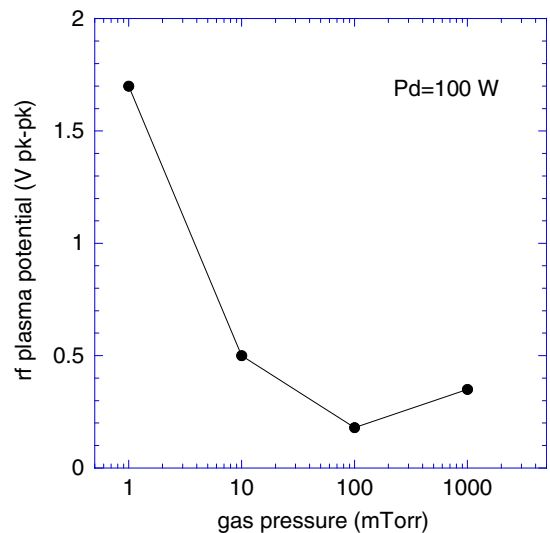**Figure 4.** Plasma rf potential versus gas pressure.

direction) is installed at the chamber axis, 3 cm from the antenna block.

The experiments were performed with argon gas in ICP with a single (outer) symmetrically driven coil at a fixed frequency of 2 MHz using a fixed matching network, as shown in figure 3.

The matching network consists of two resonating capacitors of capacitance $C = 470$ pF and a BAL-UN transmission-line step-down transformer Tr, the primary winding of which is connected to a power source G [14, 15]. The network provides a true symmetric drive with a weak detuning effect caused by the differences in the plasma load. That occurs due to the relatively small Q-factor of the antenna coil loaded with plasma.

3. Experimental results and discussions

Due to the high symmetry in the antenna coil drive, the low driving frequency and high dielectric constant (near 10) of the ceramic window, the plasma rf potential measured with a large surface probe in this ICP is extremely low, as can be seen in figure 4. Therefore, no rf probe compensation is needed for undistorted probe measurement, since the rms of the rf plasma potential, V_p, is always much less than the electron temperature ($eV_p \ll T_e$) [15, 17]. The low plasma rf potential assures

that the dc voltage in the sheath between the chamber and the plasma, as well as the dc voltage between the unbiased pedestal and the plasma, are minimal and equal to the floating potential.

Figure 5 shows the discharge electrical characteristics, the antenna coil voltage, V, and the coil current, I, as functions of the discharge power, P_d, for argon gas pressures 1; 10; 100 and 1000 mTorr. According to [17], the discharge power is calculated from the measured total transmitted power, P_{tr}, to the primary winding of the transformer ($P_{tr} = P_i - P_r$) and the antenna coil current, I, with and without plasma:

$$P_{tr} = I^2(R_0 + R_p); \qquad P_0 = I_0^2 R_0;$$
$$P_d = I^2 R_p = P_{tr} - P_0 I^2/I_0^2,$$

where P_i and P_r are the incident and reflected powers, the index 0 denotes the values measured without plasma, R_0 is the rf Ohmic resistance of the antenna coil without plasma (also accounting for power losses in the transformer, in the capacitors and in the antenna block hardware, which together are essentially less than the total power loss in the coil), R_p is the resistance transformed to the antenna due to its coupling to the plasma (hereafter called the plasma resistance) and P_d is the
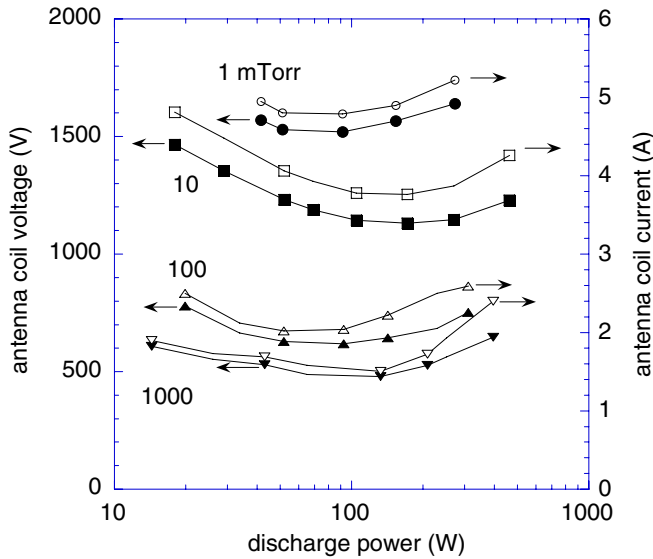
Figure 5. Antenna voltage and current versus discharge power.

Figure 6. Volt/ampere characteristic of ICP antenna loaded with plasma.
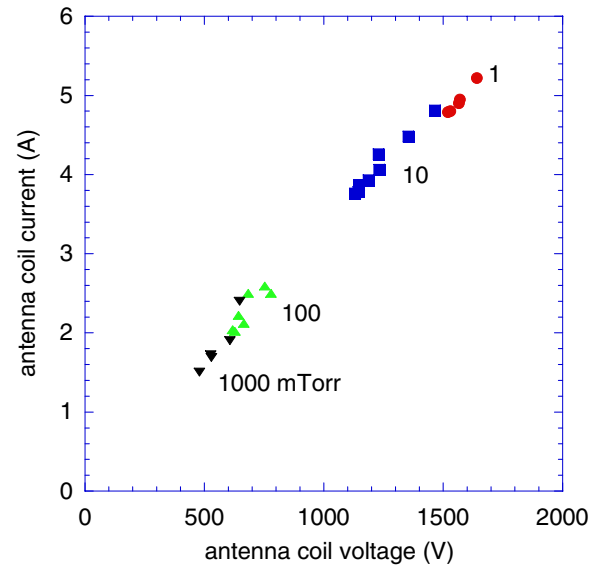
discharge power, or the power transferred to plasma electrons, the only power that is relevant to plasma-chemical processes in plasmas.

The falling dependence of the coil voltage and the coil current with respect to the discharge power seen in figure 5 looks strange and suggests decreasing discharge power for increasing coil voltage and current. Such a counterintuitive behavior of ICP electrical characteristics is due to the strong antenna-to-plasma coupling and a specific $V–A$ characteristic of non-equilibrium gas discharge plasma with a negative differential impedance $\propto dE/dJ < 0$, where E and J are the plasma rf field and current density.

The electric field that maintains the discharge (governed by ionization and electron energy balances) is a decreasing function of the plasma density. This is due to the two-step ionization and to the Maxwellizing electron–electron collisions, which both increase with plasma density. Therefore, the higher the plasma density, the lower the maintaining plasma electric field. Since in an ICP, $E \propto \omega I$ and (as shown later) the modulus of the antenna impedance Z is practically constant, both the coil current and the voltage fall similarly with the discharge power.

At a relatively high discharge power (100 W and higher), both the antenna voltage and the current increase with discharge power. Such behavior, common for ICP sources, is due to antenna leakage inductance (the part of the antenna inductance not coupled to the plasma) [16]. For an ideal coupling of the antenna to the plasma load, this effect is absent and the antenna impedance is just N^2-times larger than the impedance of the plasma current path, where N is the number of the antenna coil turns. In conventional ICPs for plasma processing with typically weak antenna coupling to plasma, the strong effect of the leakage inductance masks the effect of the plasma negative differential impedance and both the antenna voltage and the current increase monotonically with the measured total transmitted power.

As seen in figure 5, the power dependences of the antenna coil voltage and the current are similar, and the ratio between them, which is the magnitude of the antenna impedance $Z = |V|/|I| = [\omega^2(L_0 - L_p)^2 + (R_0 + R_p)^2]^{1/2}$ [16], is practically constant. Here, L_0 is the coil inductance not affected by the plasma and L_p is the reduction in the antenna inductance due to plasma conductivity [16]. In a typical ICP, $L_p \ll L_0$, $R_p^2 \ll \omega^2 L_0^2$, and therefore, $Z \approx \omega L_0$ [17]. However, at high coupling and at a high enough plasma density, which corresponds to high gas pressure and high discharge power, both L_p and R_p may affect the antenna impedance.

The plasma components of the antenna impedance ωL_p and R_p (which affect its magnitude in an opposite way) can be comparable to ωL_0, but may partly or completely compensate each other. The volt–ampere characteristic of the loaded antenna $I = I(V)$ is shown in figure 6. As one can see, for all ranges of power and argon pressures, the antenna current is nearly proportional to the antenna voltage, which corresponds to the magnitude of the antenna impedance, $Z = 308\,\Omega$, while the impedance of the unloaded antenna is $\omega L_0 = 302\,\Omega$. This means that although the plasma separately affects the Ohmic and imaginary parts of the antenna impedance, under the conditions of this experiment, the effects of the plasma on the magnitude of the antenna impedance are mutually compensated and are therefore negligible.

The transformed plasma resistance, R_p, shown in figure 7 as a function of the discharge power for different gas pressures demonstrates considerable values of R_p, accounting for up to 26 % of $Z = 308\,\Omega$. The Ohmic part, $Re(Z) = (R_0 + R_p)$, and the imaginary part, $Im(Z) = \omega(L_0 - L_p)$, of the antenna impedance define two important ICP electrical characteristics: the power factor (PF) of the antenna loaded with plasma, $\text{Cos}\,\varphi$, and the ICP power transfer efficiency (PTE), $\eta = P_d/P_{tr}$, shown in figures 8 and 9. Here,

$$\text{Cos}\,\varphi = P_{tr}/(IV) = (R_0 + R_p)/Z \qquad \text{and}$$

$$\eta = P_d/P_{tr} = R_p/(R_p + R_0).$$

Both the power factor and power transfer efficiency increase monotonically with power (plasma density) and gas pressure,
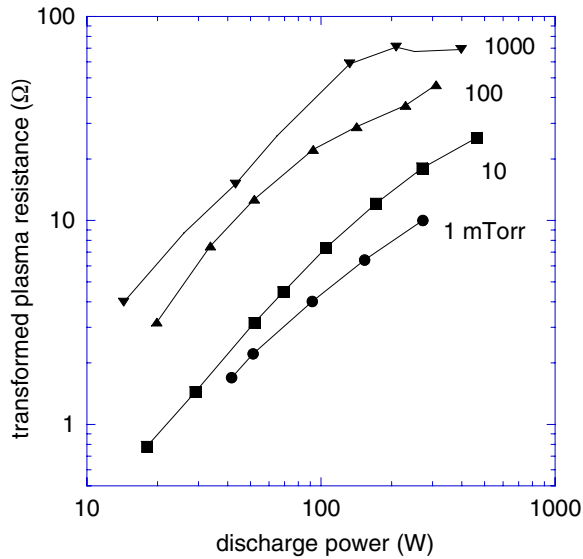
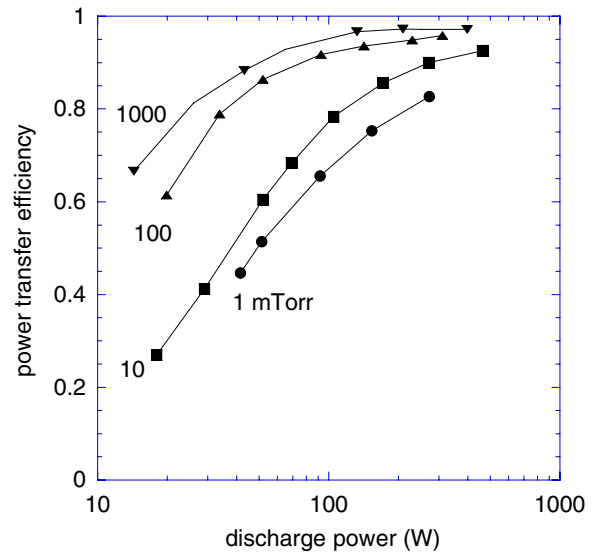**Figure 7.** Plasma resistance transferred to the antenna impedance.

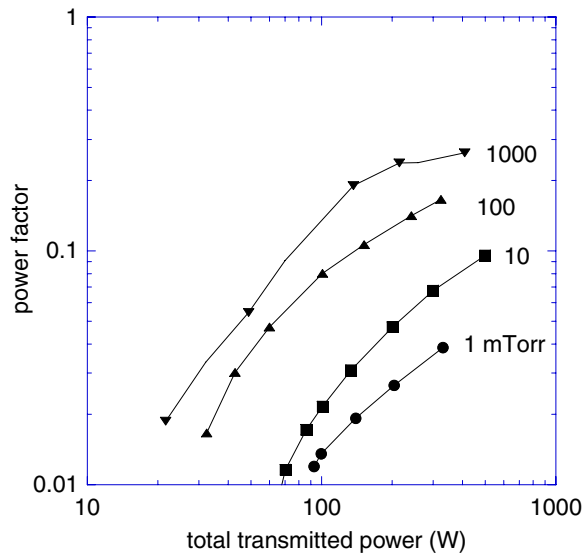**Figure 9.** ICP power transfer efficiency.

Figure 8. Antenna power factor.

and their values are considerably larger than those found in conventional ICPs of similar size and geometry [15]. The increasing antenna power factor allows one to facilitate and to simplify the matching network. An increase in power transfer efficiency is always a desirable feature. For example, in a conventional ICP design [15] at a discharge power of 200 W, argon pressure between 1 and 1000 mTorr, and driving frequencies 3.39, 6.78 and 13.56 MHz, the PTE was found to be between 0.6 and 0.8, which corresponds to 40% and 20% power loss in the antenna coil. The power transfer efficiency demonstrated in figure 9 is measured at 2 MHz, at the same power and gas pressure, and shows the corresponding numbers between 0.79 and 0.97, which corresponds to 21% and 3% power loss in the antenna together with the matching transformer. This considerable difference in the antenna power loss, which is even larger for higher discharge powers, is due to improved antenna coupling with the plasma and is achieved

by the reduction in window thickness and the application of a ferromagnetic core.

Apart from the reduction in antenna thermal loading, minimizing antenna power loss has two essential implications. Low-loss ICP antennas allow for stable ICP operation in inductive mode at low discharge powers and, thus, at low plasma densities. Empirically found rough criterion of the minimal discharge power for stable ICP operation states that the discharge power should exceed the antenna power loss $P_a = P_{tr} - P_d$, i.e. $P_d \geqslant P_a$. The opinion, widely shared in the plasma processing community, that an ICP cannot work in inductive mode at relatively small plasma densities originated from a relatively weak antenna coupling to plasma due to a thick window, and a low unloaded antenna Q-factor, Q_0, (large $R_0 = \omega L_0/Q_0$) which is affected by the proximity of the metal and by the water cooling. Stable ICP operation in inductive mode at 2.5 MHz with a discharge power of just 2 W has been demonstrated in [8]. The reduction in the window thickness also results in more local plasma electron heating near the antenna coil, thus improving spatial selectivity of the heating and the ability to control the plasma density distribution in a multi-antenna ICP. This will be considered in a future paper.

The basic plasma parameters, the electron temperature and the plasma density, were measured at the center of the discharge gap using a VGPS® [18] probe station. The electron energy distribution functions (EEDF) were measured over a wide range of argon pressures and discharge powers. The effective electron temperature $T_e = \frac{2}{3}\langle\varepsilon\rangle$ and plasma density were found as appropriate integrals of the measured EEDF [17] and are presented in figures 10 and 11.

The falling power dependence of the electron temperature at 10 mTorr and higher pressure shown in figure 10 is typical for gas discharge plasmas and is a consequence of the two-step ionization and electron–electron collisions which increase with plasma density. The reverse dependence $T_e(P_d)$ seen for 1 mTorr is associated with the preferential collisionless heating of hot electrons under the condition of the anomalous skin effect which results in the formation of a low energy peak
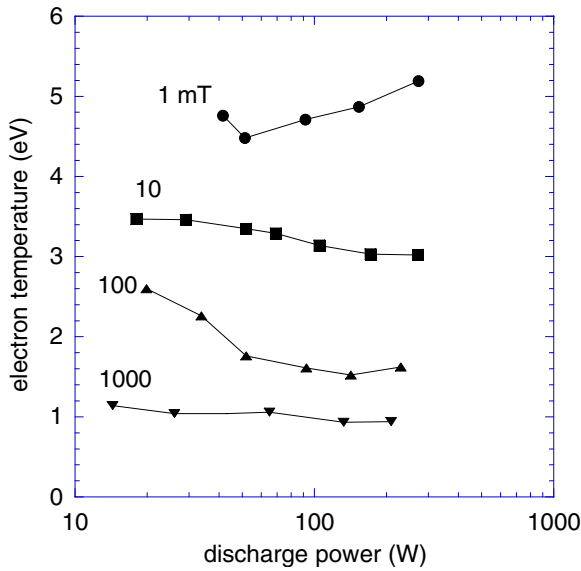
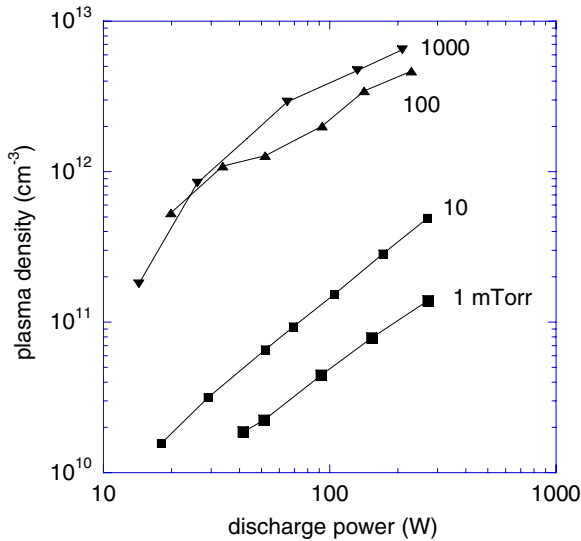**Figure 10.** Electron temperature versus discharge power.

Figure 11. Plasma density versus discharge power.

in EEDF [19]. With increasing plasma density, the electron–electron collisions tend to Maxwellize the EEDF, leading to the disappearance of the low energy peak, which results in a higher electron temperature.

The results of the plasma density measurements at the plasma center are shown in figure 11. Here one can observe a wide range of plasma density values covering almost three orders of magnitude, including a relatively low plasma density at the lowest discharge power of 15–20 W. In this experiment, the maximal values of the plasma density are limited by a limited rf power source. The ability to maintain the plasma at low rf power (low plasma density) is due to the strong coupling between the antenna and the plasma, and relatively low power loss in the antenna itself.

Experiments with different gaps, d varying between 1.5 and 8 cm, show that a stable discharge in this ICP can be maintained (except at very low gas pressures) even at the
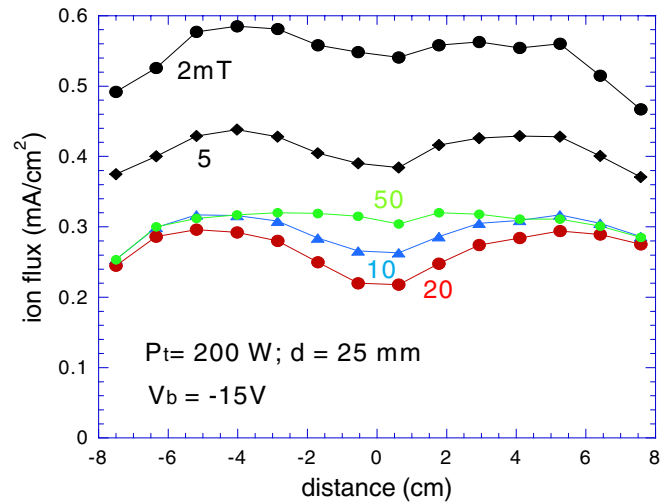

Figure 12. Ion flux profile at $d = 2.5$ cm for different gas pressures.

smallest discharge gap of 1.5 cm. A change in the discharge gap induces a variation in the plasma radial profile, starting with a diffusion-like distribution with a central maximum for large d and ending with a bi-modal distribution with a central minimum at small d.

An example of such plasma density distributions measured along the diameter of the pedestal with an array of ion collecting flat probes biased to -15 V referenced to the grounded pedestal and chamber are shown in figure 12. At $d = 2.5$ cm and $P_{tr} = 200$ W, in the range of argon pressures between 2 and 50 mTorr, the plasma density distributions have two local maxima at the radial positions a little smaller than the central radius of the antenna coil (7.5 cm). The small asymmetry in the plasma radial distribution is probably due to the gas flow along the chamber diameter to the pumping port. Plasma deficiency in its central area can be compensated with the activation of the second antenna placed near the plasma axis, as shown in figure 2.

4. Concluding remarks

An attempt to improve a 'pancake' configuration ICP by narrowing the window and reducing its surface, together with a simultaneous enhancement of its antenna performance with a ferromagnetic core, resulted in a significant improvement of the ICP electrical and plasma parameters. Lowering the operation frequency to 2 MHz and using a true balanced drive for the antenna coil resulted in practical elimination of capacitive coupling between the coil and the plasma, and thus removed all of the negative effects associated with capacitive coupling. The combination of a narrow window and a coil enhanced by a ferromagnetic core-shield has improved not only the antenna coupling to the plasma, but also the electrical characteristic of antenna itself. As a result, the antenna current was decreased, while the power transfer efficiency, η, and the antenna power factor, $\text{Cos}\,\varphi$, were essentially increased, compared with a traditional 'pancake' configuration ICP. On the other hand, a relatively low Q-factor of the antenna coil loaded with plasma, $Q = \omega(L_0 - L_p)/(R_0 + R_p) \approx (\text{Cos}\,\varphi)^{-1}$,

allowed for a simplification of the matching circuit, avoiding variable tuning elements there.

Contrary to a widely shared opinion that an ICP cannot work at low plasma densities and with a small gap, the experiments with this improved ICP have demonstrated its ability to operate over a wide range of gas pressures and plasma densities, including plasma densities considerably lower than 10^{11} cm^{-3} and gaps as narrow as 1.5 cm. The results of plasma distribution control in a multi-coil version of this ICP and EEDF measurements in argon and plasma processing gas mixture will be presented in a future paper.

Acknowledgment

References

[1] Lieberman M A and Lichtenberg A J 2005 *Principles of Plasma Discharges and Materials processing* (Hoboken, NJ: Wiley)
[2] Chen F F and Chang J P 2002 *Lecture Notes on Principles of Plasma Processing,* (New York: Kluwer/Plenum)
[3] Hershkowitz N, Ding J, Breun R A, Chen R T S, Mayer J and Quick A K 1996 *Phys. Plasmas* **3** 2197
[4] Godyak V A 2006 *IEEE Trans. Plasma Sci.* **34** 755
[5] Lieberman M A, Booth J P, Chabert P, Rax J M and Turner M M 2002 *Plasma Sources Sci. Technol.* **11** 283
[6] Chabert P 2007 *J. Phys. D: Appl. Phys.* **40** R63
[7] Chabert P, Raimbault J L, Levif P, Rax J M and Lieberman M A 2005 *Phys. Rev. Lett.* **95** 205001-04
[8] Godyak V A 2004 *Proc. 15th Int. Conf. on Gas Discharge and their Applications (Toulouse, France)* vol 2, p 621
[9] Colpo P, Meziani T and Rossi F 2005 *J. Vac. Sci. Technol.* A **23** 270
[10] Godyak V and Chung C-W 2006 *Japan. J. Appl. Phys.* **45** 8035
[11] Lim J H, Kim K N, Park J K and Yeom G Y 2008 *J. Korean Phys. Soc.* **52** 313
[12] Chen F F, Evans J D and Tynan G R 2001 *Plasma Sources Sci. Technol.* **10** 236
[13] Godyak V A 2002 *IEEE Ind. Appl. Mag.* **8** 42
[14] Rayner J P, Cheetham A D and French G N 1996 *J. Vac. Sci. Technol.* A **14** 2048
[15] Godyak V A, Piejak R B and Alexandrovich B M 1999 *J. Appl. Phys.* **85** 703
[16] Piejak R B, Godyak V A and Alexandrovich B M 1992 *Plasma Sources Sci. Technol.* **1** 179
[17] Godyak V A, Piejak R B and Alexandrovich B M 2002 *Plasma Sources Sci. Technol.* **11** 525
[18] www.plasmasensors.com
[19] Godyak V and Kolobov V 1998 *Phys. Rev. Lett.* **81** 369